Available online www.jsaer.com

***Journal of Scientific and Engineering Research*, 2017, 4(5):143-156**

Research Article

ISSN: 2394-2630
CODEN(USA): JSERBR

Beam radius effects on polycrystalline bifacial silicon solar cell electrical parameters

NZONZOLO, Désiré LILONGA-BOYENGA

Laboratoire d'Electronique et Electrotechnique, Ecole Nationale Supérieure Polytechnique, Université Marien Ngouabi, Republic of the Congo

Abstract In this paper we present results of two-dimensional analysis of a bifacial polycrystalline solar cell under Gaussian illumination, in highlighting the Gaussian beam radius effects, on the solar cell electrical parameters. The two-dimensional continuity equation with a Gaussian generation rate is solved using the finite element method. The effects of Gaussian beam radius, on the recombination and electrical parameters of the solar cell are studied namely: the carriers' density (δ), the photocurrent density (J), the short-circuit photocurrent density (Jcc), the photovoltage (V), the series resistance (Rs) and the shunt resistance (Rsh).

Keywords Solar cell, finite elements, Gaussian beam, wavelength, photocurrent, photovoltage, recombination velocity, diffusion length, shunt resistance, series résistance.

1. Introduction

To characterize solar cells, several methods are used [1-3]. Generally, these methods consist of interacting the solar cell with an external excitation, and examining the response of solar cell, namely, the photocurrent or the photovoltage produced by that one. The analysis of this response leads to determine the microscopic and macroscopic parameters which govern the solar cell working.

The solar cell illumination by a monochromatic beam not depending to its width does not take account the variability of the illumination on the solar cell surface. To take into account this variability of illumination, we propose in this study to characterize a solar cell excited by a Gaussian radiation, permitting to have a better modelling of the illumination of the solar cell surface [3]. The continuity equation which results from it will be solved using finite element method. From the evaluation of the photocurrent and the photovoltage, we will determine for various values of the Gaussian beam illumination radius, the diffusion length, the back surface recombination velocity, as well as the series resistance and the shunt resistance, starting from the electrical model of the solar cell [4, 5].

2. Theoretical analysis

Let us consider a rectangular crystal of a bifacial polycrystalline silicon solar cell having a base depth H_1, and a width H_2, as represented in figure 1.

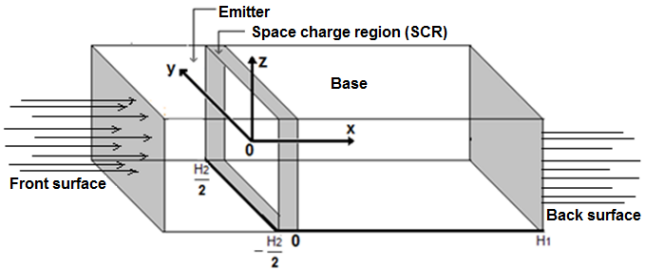

Figure 1: Rectangular Crystal of a bifacial silicon solar cell

This solar cell is illuminated by a luminous flow which we consider as a monochromatic radiation.
To carry out this study, we consider the following assumptions [5]:

- no external electric or magnetic field is applied to the semiconductor substrate;
- the influence of the semiconductor substrate thickness on the carriers' dynamics is neglected;
- the emitter contribution to the photocurrent is not taken into account.

The continuity equation which governs the solar cell's operation in this case is given as follows [5]:

$$\frac{\partial^2\delta(x,y)}{\partial x^2}+\frac{\partial^2\delta(x,y)}{\partial y^2}-\frac{\delta(x,y)}{L^2}=-\frac{g(x,y)}{D}(1)$$

where $\boldsymbol{\delta(x,y)}$ represents the photogenereted excess minority carrier's density in the base, L, the electron diffusion length, D, the diffusion coefficient. $\boldsymbol{g(x,y)}$is the generation rate. To take into account the variability of luminous flow, we suppose that this generation rate has a Gaussian form.
In these conditions, this generation rate is given by the following equation [1]:

$$\boldsymbol{g(x,y)=I_0(1-R)\alpha e^{-\alpha x}\cdot\frac{e^{-\frac{y^2}{2r_f^2}}}{2\pi r_f}}(2)$$

Where $I_0$is the illumination intensity, supposed constant. R and α are respectively, the reflexion coefficient andthe absorption coefficient on the front or the back of solar cell surface, and r_f, the radius of the Gaussian illumination.
One can note that in this relation, the classical monochromatic generation rate$g(x)=I_0(1-R)\alpha e^{-\alpha x}$ is multiplied by the corrective term $\frac{e^{-\frac{y^2}{2r_f^2}}}{2\pi r_f}$.
The continuity Equation (1) obeys to the following boundary conditions [1], namely, the current of diffusion and the current of recombination are equal on the boundaries, i.e .[5] :
- on the junction

$$\left.\frac{\partial\delta(x,y)}{\partial x}\right|_{x=0}=\frac{Sj}{D}\cdot\delta(0,y)(3)$$

- on the back surface

$$\left.\frac{\partial\delta(x,y)}{\partial x}\right|_{x=H_1}=-\frac{S_{gb}}{D}\cdot\delta(H_1,y)\ (4)$$

- on the$y=-\frac{H_2}{2}$ boundary

$$\left.\frac{\partial\delta(x,y)}{\partial x}\right|_{y=-\frac{H_2}{2}}=\frac{S_{gb}}{D}\cdot\delta\left(x,-\frac{H_2}{2}\right)(5)$$

-on the$y=\frac{H_2}{2}$ boundary

$$\left.\frac{\partial\delta(x,y)}{\partial x}\right|_{y=\frac{H_2}{2}}=-\frac{Sgb}{D}\cdot\delta\left(x,\frac{H_2}{2}\right).(6)$$

Sj indicate sthe junction recombination velocity, Sb, the back surface recombination velocity and Sgb, the boundary recombination velocity on the boundaries$y=-\frac{H_2}{2}$and$y=\frac{H_2}{2}$.

2.1. Resolution of the continuity equation by the finite element method

This continuity equation is an elliptic differential equation, which can be written to the following general form:

$$-\nabla(c\nabla u)+\beta\cdot u=f\qquad(7)$$

It obeys to the Neumann boundaries conditions [5, 7], namely:

$$\begin{cases}u_x'(0,y)=a\cdot u(0,y)\\ u_x'(H_1,y)=b\cdot u(H_1,y)\\ u_y'\left(x,-\frac{H_2}{2}\right)=c_1\cdot u\left(-\frac{H_2}{2},y\right)\\ u_y'\left(x,\frac{H_2}{2}\right)=c_2\cdot u\left(x,\frac{H_2}{2}\right)\end{cases}$$

where$c=1,\beta=\frac{1}{L^2},u=\delta(x,y),\ u_x'=\frac{\partial u}{\partial x},\ u_y'=\frac{\partial u}{\partial y}andf=\frac{g(x,y)}{D}$.

a, b, c_1 and c_2 are the constant such as :

$a = \frac{Sj}{D}$; $b = -\frac{Sb}{D}$; $c_1 = \frac{Sbg}{D}$; $c_2 = -\frac{Sgb}{D}$

The variational form associated to the equation (7) can be written as follows:

$F(u) = \frac{1}{2}\int_\Omega (\nabla u)^2 dxdy + \frac{1}{2}\int_\Omega \beta u^2 dxdy - \int_\Gamma \vec{n} \cdot u\vec{\nabla} uds - \int_\Omega f u dxdy = 0$(8)

where $\vec{n}$ is the normal unit vector on the border and $\vec{n} \cdot (\vec{\nabla} u) = \frac{\partial u}{\partial n}$, the normal derivative.

To solve equation (7), one models the crystal of the solar cell by a rectangular domain Ω, delimited by x=0 and $x=H_1$ according to ox, and $y = -\frac{H_2}{2}$ and $y = \frac{H_2}{2}$ according to oy. This domain is subdivided into triangular finite elements, with h_1, the step of the mesh according to ox, and h_2, the step according to oy [5, 8].

After minimization of the variational form (8), we obtain the equation [5]:

$AU = L$(9)

or inversely:

$U = A^{-1} L$(10)

Where A and L are the global matrix of all finite elements. The vector $U = [u_1, u_2, u_3, \ldots . u_{N+1}]$ is the unknown excess minority carrier's density and N, the node number of the mesh.

The resolution of the equation (10) then makes it possible to determine the excess minority carriers' density photogenerated [5, 9], from which the photocurrent density and the photovoltage are determined.

2.2. Generation rate

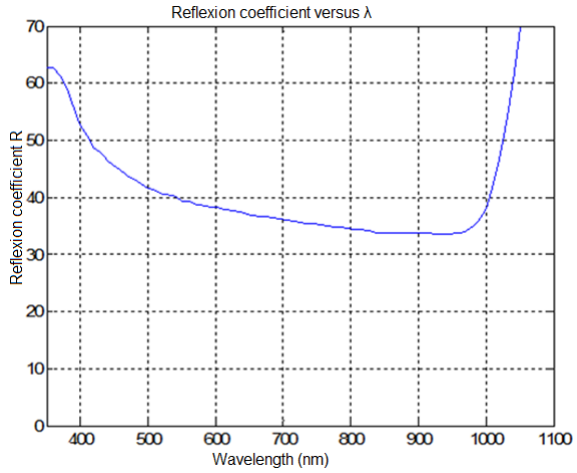

Figure 2a : Reflexion coefficient of the solar cell versus λ [1, 2].

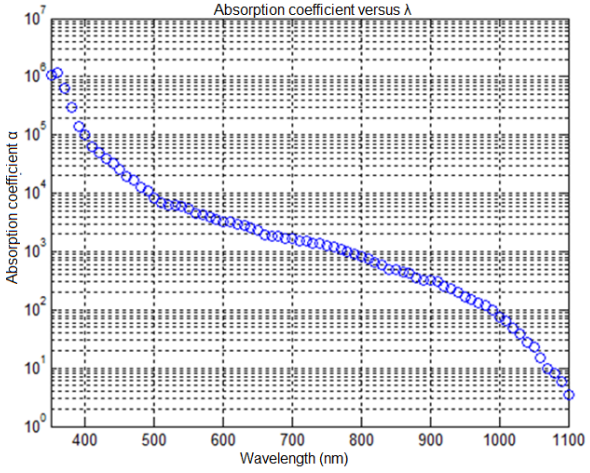

Figure 2b: Absorption coefficient of the solar cell versus λ[10].

To solve equation (9), it is necessary to know the second member *i.e* the generation rate $g(x,y)$ given by the equation (2).
In the silicon semi-conductor, this generation rate depends on the reflexion coefficient R on the solar cell surface, and the absorption coefficient ɑ. Both these parameters depend on the wavelength λ of the illumination, as represented in figures 2a and 2b [1, 2, 10].

The analysis of these curves shows that:
- the reflection is lower for the wavelengths values located between 700 and 980 nm. Thus for these values of wavelength, the incidence luminous flow absorbed by the solar cell is more important [1, 2].
- The absorption is higher when λ<365nm. It decreases when the wavelength increases [10].

2.3. Photocurrentdensity and photovoltage

The photocurrent density and the photovoltage are determined from relations (9) and (10), respectively, as follows [5]:

$$J = \frac{q \cdot D}{H_2} \int_{-\frac{H_2}{2}}^{\frac{H_2}{2}} \left[\frac{\partial \delta(x,y)}{\partial x}\right]_{x=0} dy \qquad (9)$$

$q$indicates the electron's charge and

$$V = V_T Log\left(\frac{Nb}{n_i^2} \int_{-\frac{H_2}{2}}^{\frac{H_2}{2}} \delta(0,y) dy + 1\right) \qquad (10)$$

V_T represents the thermal voltage, Nb: the doping in the base and ni, the intrinsic carrier's density.

2.4. Short-circuit photocurrent density

The photocurrent density J being constant for very large values of junction recombination velocity Sj, its derivative is equal to zero [3] [4]. This condition permits to determine the back surface recombination velocity Sb, given by [4]:

$$S_b = D \cdot \frac{\alpha\left(ch\left(\frac{H}{L}\right) - exp(-\alpha \cdot H)\right) - \frac{1}{L} sh\left(\frac{H}{L}\right)}{ch\left(\frac{H}{L}\right) - L \cdot sh\left(\frac{H}{L}\right) \cdot \alpha - exp(-\alpha \cdot H)} \qquad (11)$$

Knowing all other parameters, one can determine the short-circuitphotocurrentdensityJcc, and the photovoltage, according to the diffusion length L [4].

2.5. Macroscopic parameters of the solar cell

If we neglect the diode current, the equivalent electrical circuit of the solar cell can be illustrated as in figure 3 [4].

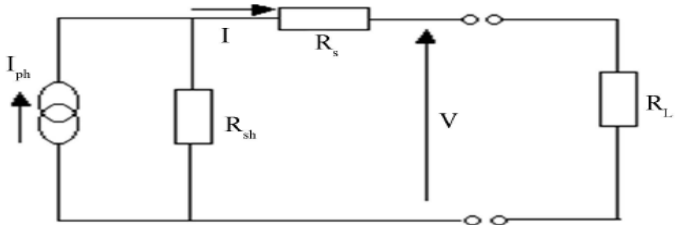

Figure 3 : Equivalent electrical circuit of the solar cell

where Iph represents the photocurent, Rs, the series resistance, Rsh, the shunt resistance, and R_L, the load resistance. These resistances are given respectively by [11]:

$$R_{sh} = \frac{V}{I_{cc} - I} \qquad (12)$$

$$R_s = \frac{V_{co} - V}{I} \qquad (13)$$

Where Icc indicates the short-circuit photocurrent density and Vco, the open circuit photovoltage.

3. Results and Discussions

To determine the microscopic and macroscopic parameters of the solar cell illuminated by a Gaussian luminous flow, it is necessary to know the generation rate of the photogenereted carriers, namely the reflexion coefficient R, and the absorption coefficient α. In this objective, while basing itself on the curves of the figures 2a and 2b giving the variations of R and α according to λ, we have represented in figure 4, the variation of the generation rate versus λ, for various values of the base depth x, with rf= 0,015 cm and y=0 corresponding to the maximum Gaussian flow.

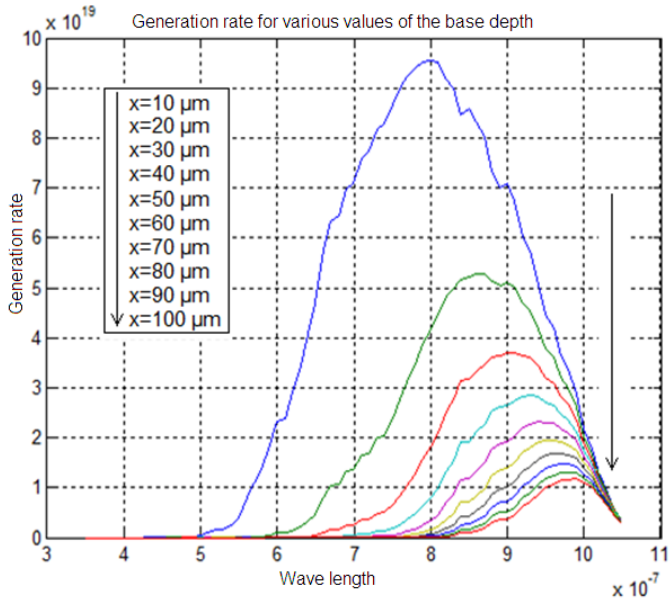

Figure 4 : Generation rate versus λfor various values of the base depth x.

These curves shows that the generation rate increases rapidly starting from 500 nm then reaches a maximum before decreasing. This maximum is higher when the value of the base depth is low. We can note that the maximum of the generation rate corresponds to x=10 µm and a wavelength value λ=800 nm. Knowing the value of λ, it is easy to deduce starting from the curves represented in figures 2a and 2b, the values of the reflection coefficient R, and the absorption coefficient α, corresponding to the maximum of the generation rate. We have found respectively $R = 0.3448$ and $\alpha = 825.8\ cm^{-1}$.

After determining the values of R and α, the generation rate given by the equation (2), is represented in figure 5, versus to the base depth x, and the grain width y, with a radius of Gaussian luminous flow, rf=300 µm.

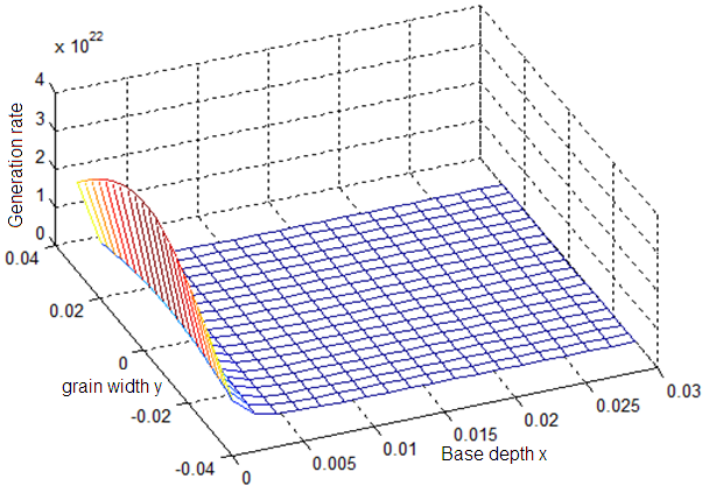

Figure 5: Generation Rate of Gaussian flow versus to the base depth and the grain width

Obviously, this generation rate is higher at the center of the solar cell grain and in the vicinity of the junction (x=0). It decreases rapidly and tends towards zero, when the base depth increases.
To illustrate the effects of the radius of luminous flow on this generation rate, we represented it in figure 6 in the vicinity of the junction, versus the grain width, for various values of the radius of Gaussian luminous flow.

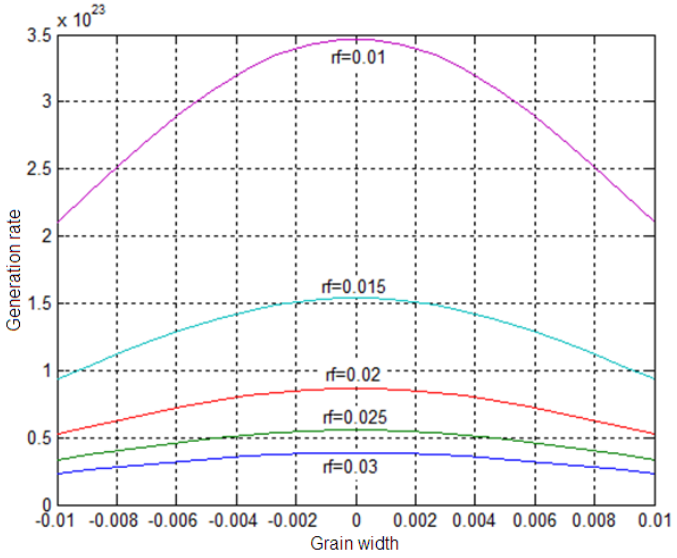

Figure 6: Generation rate versus the grain width in the vicity of junction.

one can note that the generation rate increases when the radius of the Gaussian luminous flow decreases.

3.1. Minority carriers density photogenerated

Knowing the second member of the continuity equation (1),we have solved this equation using the finite element method and determined the excess minority carriers' density which is represented in figure 7, with a radius of luminous flow rf=0.01 cm.

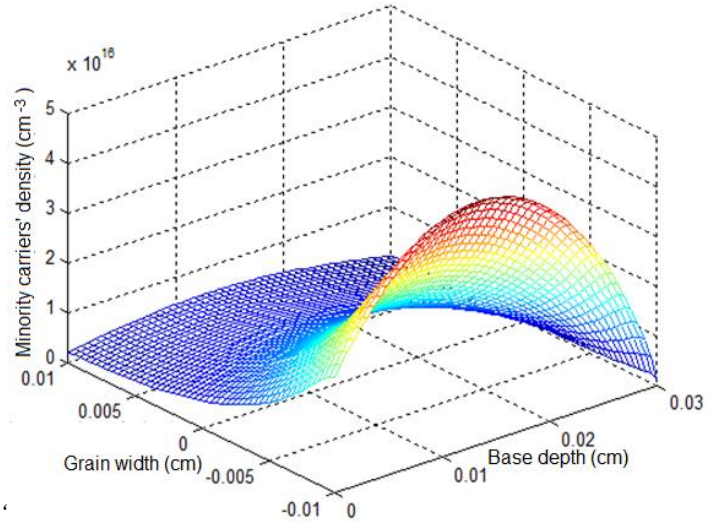

Figure 7: Minority carriers' densityversus base depth: D=26 cm^2/s; L=0.01 cm ;Sj=10^4 ; Sb=10^5 cm/s ; Sbg=10^2 cm/s.

To highlight the effect of the radius of Gaussian flow rf on the minority carriers density, we represented in figure 8, the photogenereted minority carriers' density versus the base depth for various values of rf.

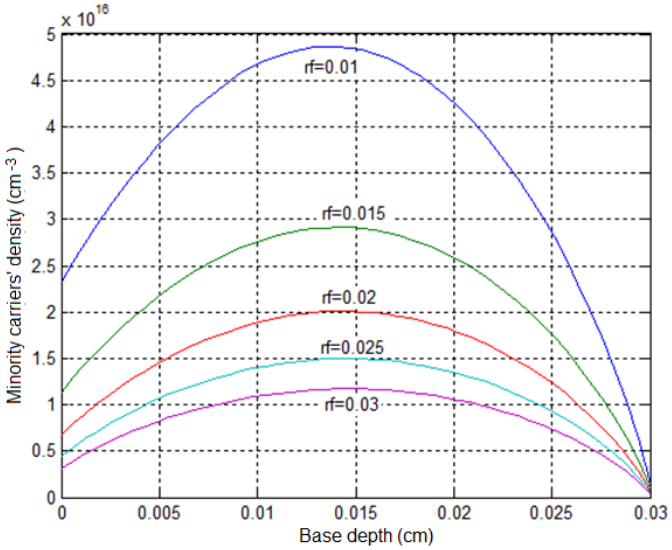

Figure 8: Minority carriers' density for various values of rf.

As shown in these curves, the minority carriers' density photogenereted by a Gaussian luminous flow, increases when the base depth increases. It reaches a maximum value and decreases in tending towards zero, when one approaches the back surface.

One can note that the minority carriers' density photogenerated by the Gaussian luminous flow, just like the generation rate, decreases when the radius of luminous flow increases. That can be due to the fact that the illumination intensity is the same for all values of rf. In fact the decrease of radius of Gaussian luminous flow involves the increase of the incidence power density, leading to the photogenerated carriers' density increase. This result is in agreement with those obtained by previous studies [6].

3.2. Photocurrent density

After obtaining the photogenerated minority carriers' density, we have determined the photocurrent density, which we represented in figure 9, versus the junction recombination velocity Sj, and the grain width of solar cell, for rf=0.01cm.

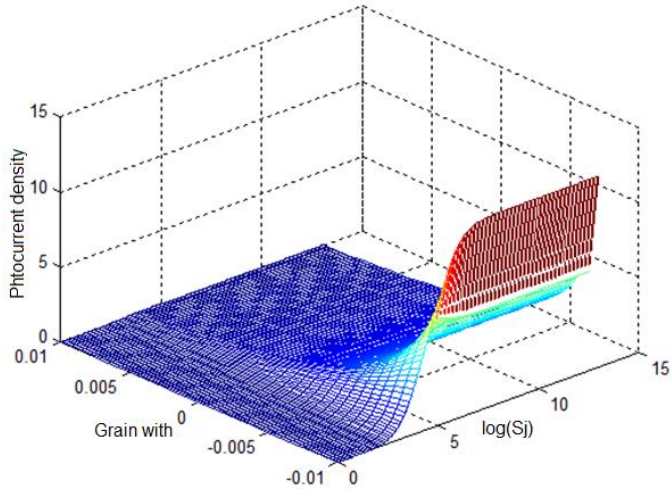

Figure 9 : Photocurrent densityversus Junction recombination velocity Sj. D=26 cm²/s; L=0.01cm; Sb=10² cm/s; Sbg=10² cm/s.

One can note that the photocurrent density is null for the small values of junction recombination velicity Sj which corresponds to the open circuit solar cell opreration. It increases when Sj increases and saturates for the great values of Sj, corresponding to the solar cell short-circuit operation.
To illustrate the effect of the Gaussian luminous flow radius on the photocurrent density, we represented it in figure 10, for various values of rf, according to junction recombination velocity Sj.

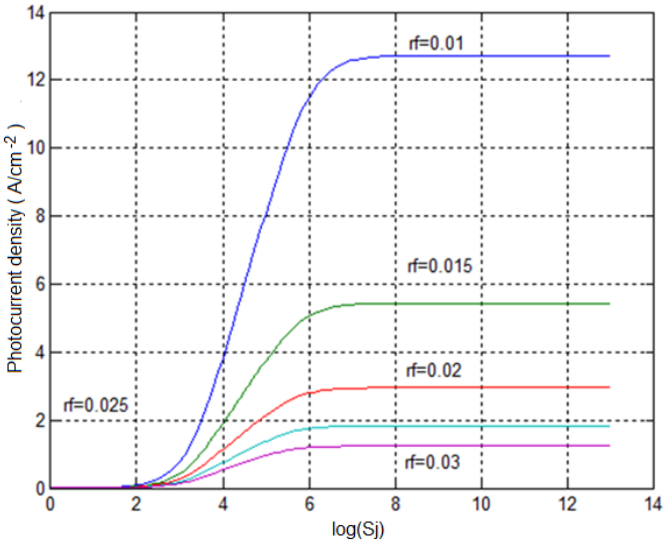

Figure 10: Photocurrent density versus junction recombination velocity Sj, for various values of rf. D=26 cm^2/s; L=0.01 cm; Sb=10^2cm/s; Sbg=10^2 cm/s.

As we noted for the minority carriers' density, the photocurrent density, decreases when Gaussian flow radius increases.

3.3. Phototovoltage

The photovoltage has been determined using our calculation code and represented according to the junction recombination velocity Sj, and the grain width of the photovoltaic cell. This curve is represented in figure 11 with a value of rf=0.01cm.

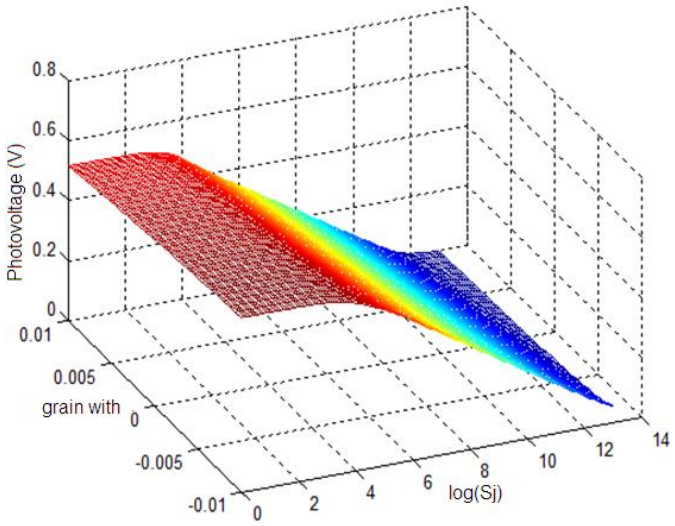

Figure 11: Photovoltage versus Sj and the grain width: D=26 cm^2/s; L=0.01 cm; Sb=10^2 cm/s; Sbg=10^2 cm/s.

We can note that for the low values of the junction recombination velocity, the photovoltage is constant. What corresponds to the solar cell open circuit working. This photovoltage decreases and then tends towards zero for the great values of Sj, *i.e.* values of Sj corresponding to the solar cell short-circuit working.

We represented in figure 12 the photovotage for various values of rf.

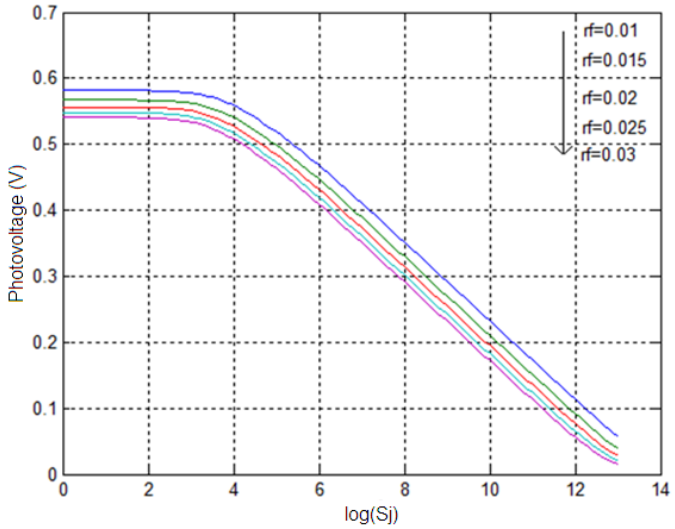

Figure 12: Photovoltage versus Sj for various values of rf. D=26 cm^2/s; L=0.01 cm;Sb=10^{2}cm/s; Sbg=10^2 cm/s.

We can also note that the open circuit photovoltage decreases when the Gaussian flow radius increases.

3.4. Current-voltage characteristic

After determining the photocurrent density and the photovoltage, we have evaluated the current-voltage characteristic and represented it versus Sj, for various values of rf. in figure 13.

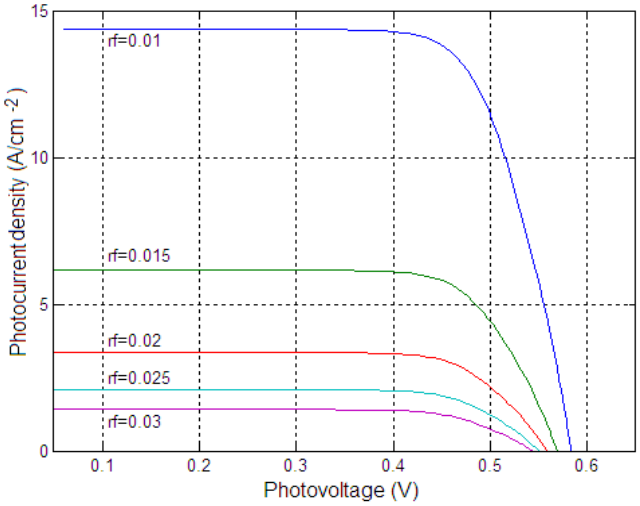

Figure 13: Current-voltage characteristic for various values of rf. D=26 cm^2/s; L=0.01 cm; Sb=10^2 cm/s; Sbg=10^2 cm/s.

These curves show that smaller is the Gaussian luminous flow radius, higher are the short-circuit photocurrent density Jcc, and the open circuit photovoltage Vco.

3.5. Short-circuit photocurrent density and Effective diffusion length

The short-circuit photocurrent density Jcc, has been deternined according to the diffusion length L, and the grain width. It is plotted in figure 14, for a value of rf=0.05cm.

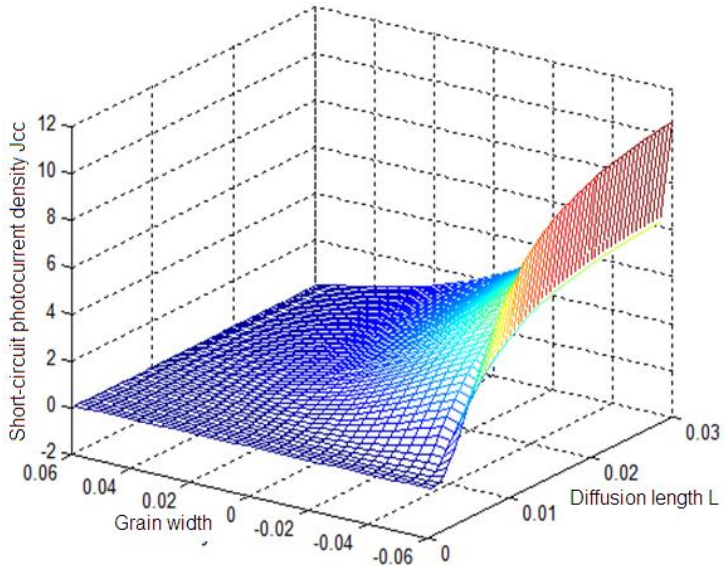

Figure 14: Short-circuit photocurrent density versus the diffusion length L. D=26 cm^2/s; Sbg=10^2 cm/s.

Let us note that for various values of rf, the short-circuit photocurrent density is represented versus L, in figure 15.

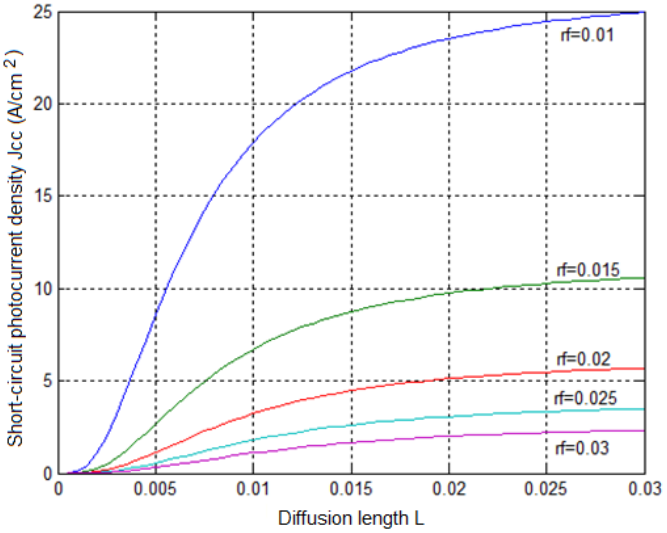

Figure 15: short-circuit photocurrent density versus L. D=26cm^2/s; Sbg=10^2 cm/s.

One notes that the short-circuit photocurrent density decreases when Gjaussian flow radius increases.
These curves enable us to determine the values of Jcc for each value of rf.
Another important microscopic parameter of the solar cell is the effective diffusion length. To determine it, we have applied the T.I.C.C.C. technic (Short-circuit Insertion Technic) [4, 14]. Actually the use of this method required to know the experimental value of the short-circuit current Jcc corresponding to the illumination used. However, to estimate the order of the magnitude of the photovoltaic cell effective diffusion lengths, we gave to Jcc the values deduced from figure 10.

The results obtained are listed in table 1.

Table 1: Recombination parameter L_{eff}

Gaussien flow radius rf (cm)	Jcc (mA)	Leff (cm)
0.010	12.7233	0.0087
0.015	05.4397	0.0042
0.020	03.9550	0.0037
0.025	01.8326	0.0025
0.030	01.2366	0.0020

Asawaited the effective diffusion lenght decreases with the increasingof the Gaussian luminous flow radius.

3.6. Shunt and series resistances

The photovoltage V and the photocurrent density being known according to the junction recombination velocity Sj, one can plot the shunt resistance Rsh and series resistance Rs, versus Sj [11].

The shunt resistance represented in figure 17 for various values of rf.

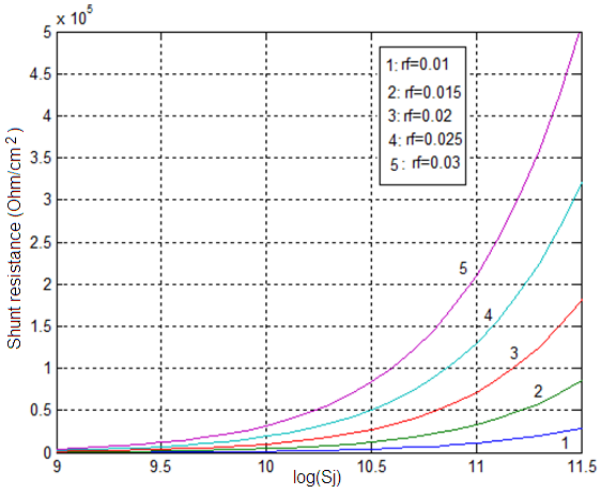

Figure 16 : Shunt resistance versus the junction recombination velocity Sj, for various values of rf.

The shunt resistance increases when the Gaussian flow radius increases. This tendency is in conformity with the results given by references [3] and [4]. This resistance being function of Sj, one can find an optimal operation point of the solar cell, corresponding to the optimal shunt resistance.

In the same way, the series resistance is represented in figure 18, for various values of rf.

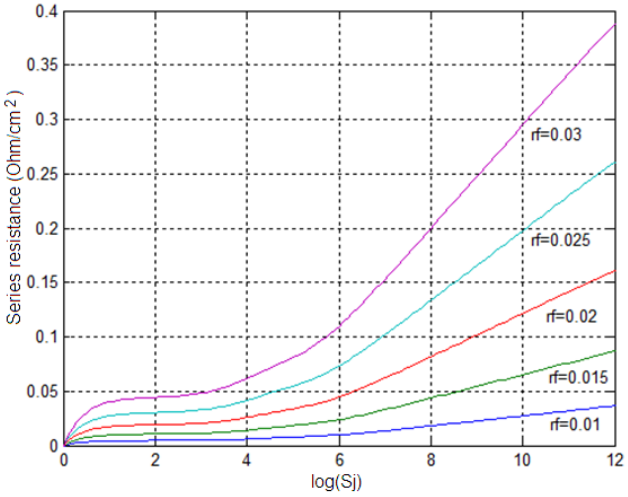

Figure 17: Series resistance versusSj, for various values of rf

3.7. Gaussian illumination effects on the solar cell electrical parameters

To highlight Gaussian illumination effects on solar cell electrical parameters, we have compared the current-voltage characteristics, the shunt and series resistance of the solar cell, when it is illuminated by a Gaussian flow and when it is illuminated by the classical monochromatic flow.

This comparative study carried out on the current-voltage characteristic is represented in figure 18.

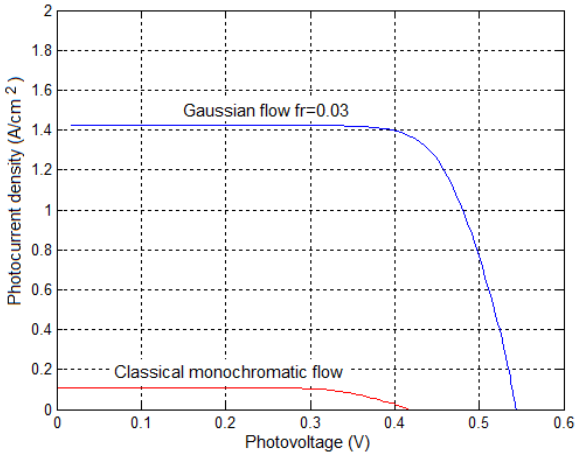

Figure 18 : Current-voltage characteristic: Gaussian and classical monochromatic flows

It shows that the photocurrent produced by the Gaussian flow is higher than that produced by the classical monochromatic flow. Same effects are observed on the shunt and series resistances, as shown in figures 18 and 19,in which these quantities are represented versus Sj.

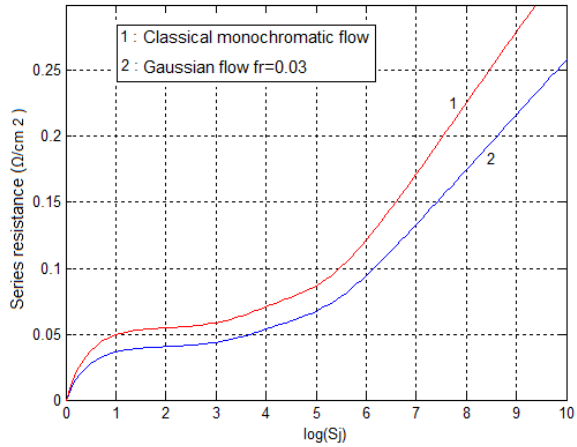

Figure 19: Series resistance: Gaussian and classical monochromatic flows

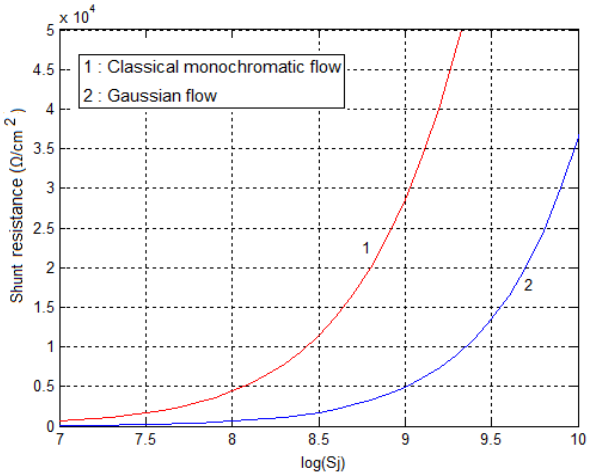

Figure 20: Shunt resistance: Gaussian and classical monochromatic flows.

Therefore, the photocurrent density resulting from the classical monochromatic flow is veryweak compared with that produced by the Gaussianflow. In addition, the photocurrent density resulting from the classical monochromatic flow and the shunt resistance are multiplied by 100 and, the series resistance by 10.
One can note that the Gaussian flow affects considerably the order of magnitude of these resistances although they preserve the same variations.

4. Conclusion

After examining the generation rate, the photgenerated minority carriers' density, the photocurrent density, the photovoltage and the short-circuit current density, we can note that when the gaussien flow radius decreases, there is improvement of the solar cell parameters resulting in the increase of the photovoltage and the photocurrent density,since the reduction in rf involves the increase in the incidental power density due to the reduce of the illumined surface of solar cell.
Thus, by acting on the Gaussian flow radius, one can improve the performances of solar cells, which can be illumined by a Gaussian flow.

References

[1]. Yassine SAYAD (2009), Détermination de la longueur de diffusion des porteurs de charge minoritaires dans le silicium cristallin par interaction lumière matière, Thèse de doctorat.Institut National des Sciences Appliquées de Lyon, France.
[2]. SAYAD Yassine (2009), Interaction Laser-Semi-conducteur: Contribution à l'étude de la technique LBIC - application au silicium photovoltaïque, Thèse de doctorat ; Université Mentouri de Constantine Faculté des Sciences Exactes Département de Physique, Algérie.
[3]. NZONZOLO (2004), Détermination des paramètres de recombinaison à partir de l'étude de la caractéristique courant-tension d'une photopile bifaciale sous éclairement constant. Thèse de doctorat troisième cycle. Université Cheikh AntaDiop de Dakar Sénégal.
[4]. Nzonzolo, D. Lilonga-Boyenga, G. Sissoko (2014). Illumination Level Effects On Macroscopic Parameters Of A Bifacial Solar Cell. *Energy and Power Engineering*, 6, 25-36.
[5]. Nzonzolo, Désiré Lilonga-Boyenga, Camille Nziengui Mabika, Grégoire Sissoko (2016). Two-Dimensional Finite Element Method Analysis Effect of the Recombination Velocity at the Grain Boundaries on the Characteristics of a Polycrystalline Silicon Solar Cell. *Circuits and Systems*, 7, 4186-4200.
[6]. S. Gueye, H. Ly. Diallo, M. Ndiaye, M. M. Dione, G. Sissoko (2013): Effect of the Boundary Recombination Velocity and the Grain Size at the Phenomenological Parameters of the Monofacial Solar Cells under Multispectral Illumination in Steady State. *International Journal of Emerging Technology and Advanced Engineering*, Volume 3, 1-8.
[7]. Daveau Christian, (2011). cours méthodes des éléments finis : Université de Cergy-Pontoise, Département de mathématique, 95302, Cergy-Pontoise, cedex France.
[8]. Matthew N. O. Sadiku (2000). Numerical Techniques in Electromagnetics. 2nd Edition, Ch.6, ISBN 0-8493-1395-3, CRC Press LLC.
[9]. Nzonzolo, Desire Lilonga-Boyenga, Camille N. Mabika, and Gregoire Sissoko (2017). Characterization of a Bifacial Silicon Solar Cell Under Multispectral Steady State Illumination Using Finite Element Method, *Progress In Electromagnetics Research M*, Vol. 53, 131–140.
[10]. Anne Kaminski, Mathieu Monville, Cours, Energie photovoltaïque Filière Physique desComposants Nanostructurés PHELMA –Septembre 2010. INP Grenoble -INSA Lyon Solarforce, France.
[11]. M.A. Ould El Moujtaba, M. Ndiaye, A. Diao, M. Thiame, I.F. Barro and G. Sissoko (2012). Theoretical Study of the Influence of Irradiation on a Silicon Solar Cell Under Multispectral Illumination. Research Journal of Applied Sciences, Engineering and Technology 4 (23): 5068-5073.
[12]. Fakoro Souleymane Dia, Ousmane Diasse, Raguilnaba Seydou Sam, Hawa Ly Diallo, Biram Dieng, Ndeye Thiam, Senghane Mbodji, Gregoire Sissoko (2012),1D Modeling Study of Series and Shunt

Resistances of Silicon Solar Cell in Steady State Operating Condition and under Polychromatic Illumination. *International Journal of Advanced Technology & Engineering Research (IJATER)*, Volume 2, 18-25.

[13]. I. Ly, O.H. Lemrabott, B. Dieng, I. Gaye, S. Gueye, M.S. Diouf and G. Sissoko. (2012). Techniques de détermination des paramètres derecombinaison et le domaine de leur validitéd'une photopile bifaciale au silicium polycristallin souséclairement multi spectral constant en régime statique. *Revue des Energies Renouvelables*, Vol. 15 N°2 187 – 206.

[14]. G. Sissoko, E. Nanéma, A. Corréa, P.M. Biteye, M. Adj, A.L. Ndiaye (1998). World Renewable Energy Congress, pp.1848-1851.